Mechanical Stress Signaling in Pancreatic Cancer Cells Triggers p38 MAPK- and JNK-Dependent Cytoskeleton Remodeling and Promotes Cell Migration via Rac1/cdc42/Myosin II

Maria Kalli[1], Ruxuan Li[2], Gordon B. Mills[3], Triantafyllos Stylianopoulos[1], and Ioannis K. Zervantonakis[2,4]

ABSTRACT

Advanced or metastatic pancreatic cancer is highly resistant to existing therapies, and new treatments are urgently needed to improve patient outcomes. Current studies focus on alternative treatment approaches that target the abnormal microenvironment of pancreatic tumors and the resulting elevated mechanical stress in the tumor interior. Nevertheless, the underlying mechanisms by which mechanical stress regulates pancreatic cancer metastatic potential remain elusive. Herein, we used a proteomic assay to profile mechanical stress–induced signaling cascades that drive the motility of pancreatic cancer cells. Proteomic analysis, together with selective protein inhibition and siRNA treatments, revealed that mechanical stress enhances cell migration through activation of the p38 MAPK/HSP27 and JNK/c-Jun signaling axes, and activation of the actin cytoskeleton remodelers: Rac1, cdc42, and myosin II. In addition, mechanical stress upregulated transcription factors associated with epithelial-to-mesenchymal transition and stimulated the formation of stress fibers and filopodia. p38 MAPK and JNK inhibition resulted in lower cell proliferation and more effectively blocked cell migration under mechanical stress compared with control conditions. The enhanced tumor cell motility under mechanical stress was potently reduced by cdc42 and Rac1 silencing with no effects on proliferation. Our results highlight the importance of targeting aberrant signaling in cancer cells that have adapted to mechanical stress in the tumor microenvironment, as a novel approach to effectively limit pancreatic cancer cell migration.

Implications: Our findings highlight that mechanical stress activated the p38 MAPK and JNK signaling axis and stimulated pancreatic cancer cell migration via upregulation of the actin cytoskeleton remodelers cdc42 and Rac1.

Introduction

Pancreatic ductal adenocarcinoma (PDAC) is responsible for over 90% of pancreatic cancer cases and is the seventh leading cause of cancer-related death in the United States (1). PDAC is characterized by extremely poor prognosis with a 5-year survival rate of less than 8% (1). New treatments for pancreatic cancer are urgently needed as it is highly resistant to all current chemotherapy and radiotherapy approaches. Complete surgical resection is currently the only curative treatment; however, patients with advanced or metastatic pancreatic cancer are most often ineligible for surgical removal, and even following resection, the tumor usually relapses within a year after surgery (1).

Current studies focus on normalizing the microenvironment of PDACs (2, 3). The PDAC microenvironment is characterized by a dense tumor-associated stroma composed of extracellular proteins, such as collagen I and hyaluronan that are remodeled to create a stiff extracellular matrix, a condition known as desmoplasia (4–6). Losartin, through its transforming growth factor beta (TGFβ) inhibitory activity, has been tested in the clinic as an approach to target the dense stroma (7). Increased matrix stiffness also serves as a diagnostic marker and is associated with poor prognosis. It can activate focal adhesion proteins, such as focal adhesion kinase (FAK) and paxillin, and actin cytoskeleton remodelers, such as RAC, RHO GTPase/Rho-associated kinase (ROCK) and RAS GTPases, to trigger signaling cascades that induce cell motility, migration, and invasion (8, 9). Moreover, tumor growth within a physically restricted environment also leads to the development of mechanical compressive forces in the tumor interior, resulting in intratumoral compressive stresses that can reach up to 75 mmHg (10 kPa; refs. 3, 10, 11). This type of mechanical stress has been shown to activate signaling pathways that promote tumorigenesis and invasiveness (12–14). However, the molecular mechanisms that underly the effects of mechanical stress on metastatic potential remain elusive.

We hypothesized that mechanical stress activates signaling pathways shown to be consistently activated in pancreatic tumors. These pathways include the PI3K/AKT and RAS/MAPK signaling cascades that are involved in the regulation of cell survival and motility (3). The increased RAS/MAPK signaling is likely due to K-Ras being the most frequently mutated gene in invasive pancreatic tumors with a rate of 95% (3). K-Ras can activate the PI3K/AKT pathway, but its main target is the MAPK signaling cascade, that includes the c-Jun N-terminal kinase (JNK) and p38 mitogen-activated protein kinase (p38 MAPK). These kinases are normally activated by environmental and genotoxic

[1]Cancer Biophysics Laboratory, Department of Mechanical and Manufacturing Engineering, University of Cyprus, Nicosia, Cyprus. [2]Department of Bioengineering, University of Pittsburgh, Pittsburgh, Pennsylvania. [3]Knight Cancer Institute, Oregon Health Sciences University, Oregon, Pennsylvania. [4]UPMC Hillman Cancer Center, Pittsburgh, Pennsylvania.

Note: Supplementary data for this article are available at Molecular Cancer Research Online (http://mcr.aacrjournals.org/).

M. Kalli and R. Li contributed equally to this article.

Corresponding Authors: Ioannis K. Zervantonakis, Department of Bioengineering, University of Pittsburgh, Pittsburgh, PA 15219. E-mail: ioz1@pitt.edu; and Triantafyllos Stylianopoulos, Department of Mechanical and Manufacturing Engineering, University of Cyprus, Nicosia, Cyprus. E-mail: tstylian@ucy.ac.cy

Mol Cancer Res 2022;20:485–97

doi: 10.1158/1541-7786.MCR-21-0266

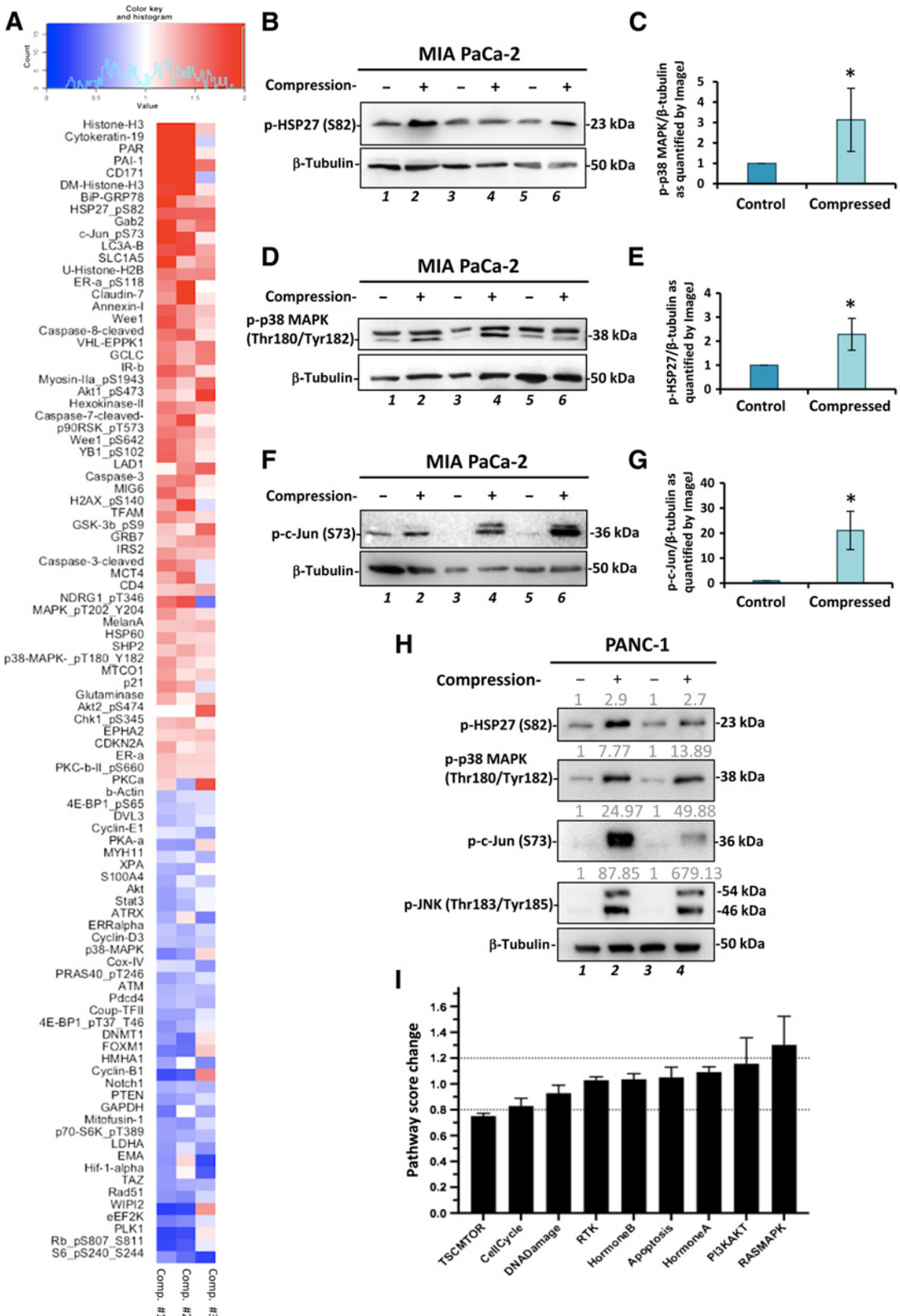
A
Color key and histogram
Count
Value
Histone-H3
Cytokeratin-19
PAR
PAI-1
CD171
DM-Histone-H3
BiP-GRP78
HSP27_pS82
Gab2
c-Jun_pS73
LC3A-B
SLC1A5
U-Histone-H2B
ER-a_pS118
Claudin-7
Annexin-I
Wee1
Caspase-8-cleaved
VHL-EPPK1
GCLC
IR-b
Myosin-IIa_pS1943
Akt1_pS473
Hexokinase-II
Caspase-7-cleaved-
p90RSK_pT573
Wee1_pS642
YB1_pS102
LAD1
Caspase-3
MIG6
H2AX_pS140
TFAM
GSK-3b_pS9
GRB7
IRS2
Caspase-3-cleaved
MCT4
CD4
NDRG1_pT346
MAPK_pT202_Y204
MelanA
HSP60
SHP2
p38-MAPK-_pT180_Y182
MTCO1
p21
Glutaminase
Akt2_pS474
Chk1_pS345
EPHA2
CDKN2A
ER-a
PKC-b-II_pS660
PKCa
b-Actin
4E-BP1_pS65
DVL3
Cyclin-E1
PKA-a
MYH11
XPA
S100A4
Akt
Stat3
ATRX
ERRalpha
Cyclin-D3
p38-MAPK
Cox-IV
PRAS40_pT246
ATM
Pdcd4
Coup-TFII
4E-BP1_pT37_T46
DNMT1
FOXM1
HMHA1
Cyclin-B1
Notch1
PTEN
GAPDH
Mitofusin-1
p70-S6K_pT389
LDHA
EMA
Hif-1-alpha
TAZ
Rad51
WIPI2
eEF2K
PLK1
Rb_pS807_S811
S6_pS240_S244
Comp. #1
Comp. #2
Comp. #3
B
MIA PaCa-2
Compression-
p-HSP27 (S82)
β-Tubulin
23 kDa
50 kDa
1 2 3 4 5 6
C
p-p38 MAPK/β-tubulin as quantified by ImageJ
Control
Compressed
D
MIA PaCa-2
Compression-
p-p38 MAPK (Thr180/Tyr182)
β-Tubulin
38 kDa
50 kDa
1 2 3 4 5 6
E
p-HSP27/β-tubulin as quantified by ImageJ
Control
Compressed
F
MIA PaCa-2
Compression-
p-c-Jun (S73)
β-Tubulin
36 kDa
50 kDa
1 2 3 4 5 6
G
p-c-Jun/β-tubulin as quantified by ImageJ
Control
Compressed
H
PANC-1
Compression-
1 2.9 1 2.7
p-HSP27 (S82)
23 kDa
1 7.77 1 13.89
p-p38 MAPK (Thr180/Tyr182)
38 kDa
1 24.97 1 49.88
p-c-Jun (S73)
36 kDa
1 87.85 1 679.13
p-JNK (Thr183/Tyr185)
54 kDa
46 kDa
β-Tubulin
50 kDa
1 2 3 4
I
Pathway score change
TSCMTOR
CellCycle
DNADamage
RTK
HormoneB
Apoptosis
HormoneA
PI3KAKT
RASMAPK

stresses and play key roles in the regulation of cell proliferation, survival, and migration. Although it less clear, they could also contribute to mechanical stress–induced signal transduction (15). In our previous studies, we showed that mechanical stress promotes growth differentiation factor 15 (GDF15)-induced cancer cell migration through activation of PI3K/AKT and MEK1/ERK1 signaling cascades in pancreatic and brain cancer cell lines, respectively (16, 17). On the basis of these findings, we used a proteomic assay to identify mechanical stress–induced signaling cascades that could contribute to motility of pancreatic cancer cells. Our results elucidate mechanical stress–induced signaling mechanisms and identify therapeutic targets to limit pancreatic cancer cell migration.

Materials and Methods

Antibodies

Antibodies against phospho-heat shock protein 27 (HSP27) (S82) and phospho-c-Jun (S73) were obtained from Abcam, while phospho-JNK (T183/Y185) and phospho-p38 MAPK (T180/Y182), were obtained from Cell Signaling Technology. Antibodies against cell division cycle 42 (cdc42) and Rac family small GTPase 1 (Rac1) were obtained from Santa Cruz Biotechnology, Inc. Antibody against β-actin was obtained from Sigma-Aldrich and anti-β-tubulin from Developmental Studies Hybridoma Bank (DSHB). For the immunofluorescence staining, phalloidin was obtained from Biotium, phospho-myosin II (Ser1943) from Cell Signaling Technology and Ki67 from Abcam.

Cell lines

MIA PaCa-2 and PANC-1 were purchased from the ATCC. Cells were grown in DMEM supplemented with 10% FBS, 1% antibiotic/antimycotic, and incubated in a CO_2 incubator at 37°C. Experiments were conducted using cells from passage 10–18. MIA PaCa-2 and PANC1 were purchased from ATCC in late 2019 and have not been authenticated since then. Cells used in this study were not subjected to *Mycoplasma* testing.

Application of mechanical stress

For the application of a defined and controlled compression (4.0 mmHg) on cancer cells, a previously described transmembrane pressure device was employed (16, 18). Twenty-four hours prior to compression, the culture medium was switched to 2% FBS-containing medium. A piston with adjustable weight was added on the top of a cell monolayer covered with an agarose cushion and placed in a transwell insert, to apply 4.0 mmHg of compressive stress for 16 hours. Control cells were covered with an agarose cushion only.

Protein extraction for reverse phase protein array

MIA PaCa-2 pancreatic cancer cells were compressed by 0.0 or 4.0 mmHg in 2% FBS-containing medium for 16 hours and washed twice with cold PBS. Cells were then lysed using 150 μL of cold lysis buffer containing 50 mmol/L HEPES, 150 mmol/L NaCl, 1.5 mmol/L $MgCl_2$, 1 mmol/L EGTA, 10% glycerol, and freshly added 1× Halt Protease Inhibitor Cocktail (Thermo Fischer Scientific), 1 mmol/L Na_3VO_4, 100 mmol/L NaF, 10 mmol/L sodium pyrophosphate, and 1% Triton-X. Cell lysates were then centrifuged at 14,000 rpm for 15 minutes at 4°C, and supernatants were collected and mixed with 4× sample buffer containing 40% glycerol, 8% SDS, 0.25 mol/L Tris-HCl pH 6, and 10% beta-mercaptoethanol (3:1). Finally, lysates were boiled at 95°C for 5 minutes and kept at −80°C. Proteomic analysis using RPPA was performed at the reverse phase protein array (RPPA) core facility (MD Anderson Cancer Center, Houston, TX).

Computational analysis: RPPA, RNA sequencing, and survival analysis

For the RPPA analysis, pairwise *t* test was performed to identify proteins that are differentially expressed between compressed and uncompressed cells. Differences are considered significant when $P < 0.05$. To visualize the protein expression patterns of compressed and uncompressed MIA PaCa-2 cells, heatmaps were generated with the *gplots* R-package. Proteins that showed significance in the paired *t* test were included in the heatmap. Heatmaps included proteins sorted on the basis of their fold change (compressed/control). For *pathway analysis*, scores were used to evaluate the activity of the pathways after compression. Pathway scores were calculated as the average weighted (positive or negative) sum of expression level of all members in each pathway (19, 20) and normalized to the uncompressed expression level. Members of nine pathways are showed in Supplementary Fig. S2. Heatmaps for pathways were generated to show the compression-induced $\log_2$ ratio of each protein member. Gene ontology enrichment analysis for RNA expression datasets from normal cells (GSE109167 mesenchymal stem cells and GSE112122 ligament cells) was performed using the *clusterprofiler* R-package. Kaplan–Meier plots for RPPA and RNA sequencing (RNA-seq) data from The Cancer Genome Atlas dataset (21) were analyzed using the *survival* R package. The code for these analyses is available as a Code Ocean compute capsulate in: https://codeocean.com/capsule/7684301/tree/v1.

Cell treatments

To examine the role of p38 MAPK and JNK in the migratory ability of pancreatic cancer cells under 4.0 mmHg stress, MIA PaCa-2 and PANC-1 cells were grown in 2% FBS-containing

Figure 1.

A RPPA was performed to reveal the mechanical stress–induced mechanism in pancreatic cancer cell lines. **A,** Heatmap showing proteins exhibiting the largest fold increases (red) or decreases (blue) in compressed MIA PaCa-2 pancreatic cancer cells relative to the control cells. Proteins were analyzed by RPPA and paired *t* test was performed to identify proteins that are differently expressed between compressed and uncompressed cells. Values in the heatmap represent the $\log_2$ ratio (compressed/uncompressed) of expression level for each protein in each condition (three biological replicates representing three columns). Differences were considered significant with $P < 0.05$. Immunoblotting was performed using the same lysates (MIA PaCa-2) that were analyzed by RPPA, to validate the activation of phospho-HSP27 (S82; **B** and **C**), phospho-p38 MAPK (Thr180/Tyr182; **D** and **E**) and phospho-c-Jun (S73; **F** and **G**) Graphs represent the average fold change ±SE in each lane normalized to β-tubulin between control and compressed cells as quantified by ImageJ (three biological replicates; $n = 3$). Asterisks (*) indicate statistically significant changes between control and compressed cells ($P < 0.05$ in Student *t* test). **H,** Validation of phospho-HSP27, -p38 MAPK, -c-Jun and -JNK, in PANC-1 pancreatic cancer cells from two biological replicates. Numbers in gray font indicate the fold change between control and compressed cells as quantified by ImageJ. **I,** Pathway score analysis was calculated as the average sum of expression level of all members in each pathway, and then normalized to the uncompressed expression level. The protein members of the pathways are shown in Supplementary Fig. S2.

DMEM for 24 hours and were then pretreated with 15 μmol/L of p38 MAPK inhibitor (SB202190, MedChemExpress) or JNK inhibitor (SP600125, MedChemExpress) for 1 hour. Control cells were pretreated with equal volume of solvent (DMSO). The concentration of each inhibitor was selected on the basis of previously published studies employing pancreatic cancer cells (22–24). Mechanical stress (4.0 mmHg) was then applied on cells growing in 2% FBS-containing medium in the presence of the inhibitors for 16 hours.

Transient transfection of pancreatic cancer cells with siRNAs

To determine whether the Rac1 or cdc42 small GTPases are implicated in the mechanical migration of pancreatic cancer cells, cells were treated with stealth siRNA (negative control, Invitrogen), siRac1, sicdc42, siJNK1, siJNK2, and sip38 MAPKα (Invitrogen) using Lipofectamine 2000 transfection reagent (Invitrogen) for 24 hours according to the manufacturer's guidelines. Cells were then washed twice with PBS and medium was switched to 2% FBS-containing medium for another 24 hours. Finally, mechanical stress was applied as described above for 16 hours.

RNA isolation and real-time PCR

Total RNA was extracted from cancer cells as described previously (18). Briefly, RNA extraction was accomplished using TRIzol (Invitrogen). RNA was then transcribed to cDNA using Superscript III Reverse Transcriptase (Invitrogen) and cDNA (1:10) was employed for quantification of gene expression by real-time PCR using β-actin as a reference gene. All primers used are shown in Supplementary Table S1. Quantification of relative gene expression was performed using the $\Delta\Delta C_t$ method, where data were log transformed and analyzed using standard methodology.

Protein extraction and Western blot analysis and quantification

For protein expression analysis, a standard immunoblotting protocol was followed as described previously (16, 17). Immunoblotting images were analyzed in Adobe Photoshop. Images were converted to grayscale. In some cases, contrast was used in the entire blot to enhance image clarity. No other image manipulation was performed. Uncropped images of immunoblotting used in this article can be found in Supplementary Materials and Methods.

Wound healing

A wound healing assay was performed on cancer cells according to previous studies (16). In brief, cells were grown to form a monolayer and then culture medium was switched to 2% FBS containing medium for 24 hours. A scratch was then introduced on the cell monolayer and mechanical compression was applied. Images from at least four different fields per condition were taken at 0 and 16 hours. The cell-free area was quantified using the ImageJ software. Quantification was performed for each condition using the following formula:

(Width of the wound at 0 hours − Width of the wound at 24 hours)/(Width of the wound at 0 hours).

Immunofluorescence staining

To determine the effect of mechanical stress on cell shape and proliferation, cells were fixed in 4% paraformaldehyde, permeabilized in PBS containing 0.25% Triton X-100 and blocked with PBS containing 0.1% Tween-20 and 1% BSA. Cells were then stained with phalloidin or anti-Ki67 antibody diluted in blocking buffer for 30 minutes or 1 hour, respectively, at room temperature. Alexa 488-goat anti-rabbit antibody was used as a secondary antibody for anti-Ki67. Images were obtained using a fluorescent microscope (Olympus BX53). For image analysis, the calculation of Ki67 area fraction was performed automatically using a previously developed in-house code in MATLAB (MathWorks, Inc.; refs. 5, 10, 11).

G-LISA assays

To examine whether Rac1 and cdc42 small GTPases are activated in response to mechanical stress, the Rac1 and cdc42 Small GTPase Activation Assay kits (G-LISA) were used (027BK127-S, 027BK128-S, Cytoskeleton, Inc) following the company's guidelines.

Statistical analysis

Results are represented as mean ± SE. Significant changes were determined by Student *t* test using two-tail distribution. If more than two groups were compared, one-way ANOVA followed by *post hoc* analysis was performed. Differences with $P < 0.05$ were considered as significant (indicated by an asterisk *).

Data availability

The RPPA data generated in this study are publicly available in Figshare.

Results

Proteomic profiling reveals heterogeneous responses across multiple pathways and uncovers activation of p38 MAPK/HSP27 and JNK/c-Jun as a mechanical stress–induced signaling pathway in pancreatic cancer cells

To profile the mechanical stress–induced signaling pathway adaptation in pancreatic cancer cells, we analyzed total and phosphorylated protein levels following application of a compressive force on pancreatic cancer cells. MIA PaCa-2 and PANC-1 cell lines carry a *KRAS* mutation, which is the most common genetic alteration found in PDAC (Supplementary Fig. S1; ref. 21). To this end, compression was first applied on MIA PaCa-2 cells at 4.0 mmHg, using a previously employed transmembrane pressure device (16) that is widely used for studying the effects of mechanical stress on cells *in vitro*. After compression, 425 proteins including phosphoproteins were assessed using RPPAs, from which 95 resulted in a statistically significant change in the compressed compared with the uncompressed cells. Proteins with the largest fold change (20%) increases (red) or decreases (blue) between control and compressed cells were visualized in a heatmap (**Fig. 1A**; Supplementary Fig. S2). We found that mechanical stress activated a number of regulators that mediate cellular adaptation to multiple stress signals, including heat shock stress, endoplasmic reticulum stress, inflammatory stress, and oxidative stress. Specifically, the cellular stress response mediator, heat shock protein 27 (HSP27_pS82) and its upstream activator p38 Mitogen-Activated Protein Kinase (p38 MAPK_pT180_Y182), exhibited a strong activation in compressed compared with control cells, that was also validated through immunoblotting in both MIA PaCa-2 and PANC-1 cells (**Fig. 1B**, **C**, **E**, and **H**). In line with p38 MAPK activation, we found that the downstream target of the stress response protein c-Jun JNK, c-Jun (pS73), was also activated in compressed cells. Subsequently both c-Jun and JNK activation were validated through immunoblotting (**Fig. 1F**–**H**; Supplementary Fig. S3). Additional markers of cellular stress, including the microtubule-associated proteins 1A/1B light chain 3B (LC3) A-B, a marker of autophagosomes, and the endoplasmic reticulum (ER) stress sensor chaperone immunoglobulin heavy chain-binding protein (BiP)-glucose regulated protein (GRP78) (also known as HSP 70), were elevated in response to compression (**Fig. 1A**).

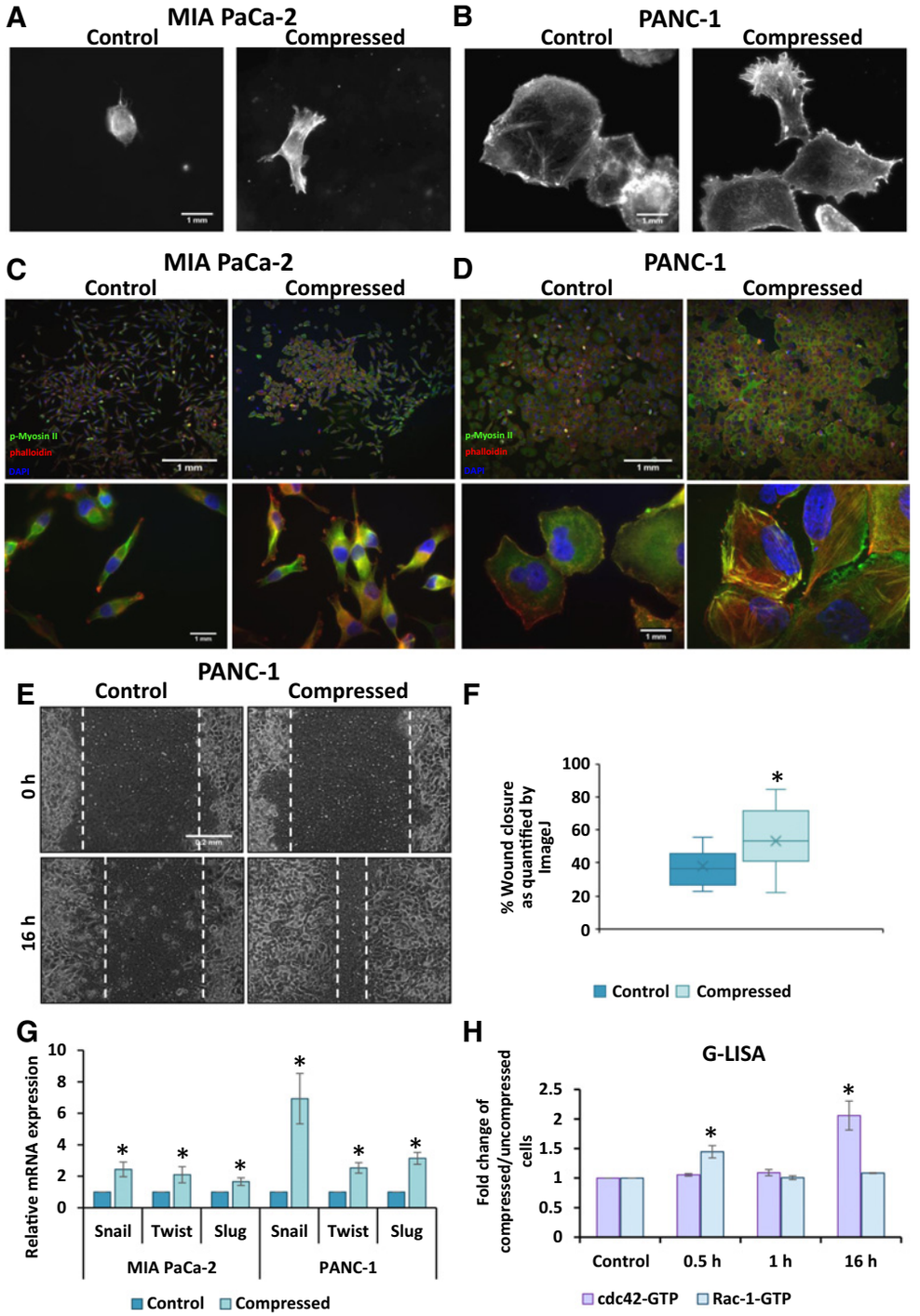

Figure 2.

Mechanical stress induces cytoskeletal changes and cell contraction in pancreatic cancer cells promoting their migratory ability. Phalloidin staining was performed to monitor cell shape, actin cytoskeleton organization of control (0 mmHg) and compressed (4 mmHg) MIA PaCa-2 (**A**) and PANC-1 (**B**) cancer cells. Scale bar 0.1 mm. Staining for phospho-myosin II (Ser1943) was performed to show actomyosin contractility in control and compressed MIA PaCa-2 (**C**) and PANC-1 (**D**) cells. Scale bar 1 and 0.1 mm, respectively. **E,** PANC-1 cells were compressed by 4.0 mmHg in low-serum medium and then subjected to a scratch wound healing assay for 16 hours. Control cells (0 mmHg) were compressed by an agarose cushion only. Scale bar: 0.2 mm. **F,** Graph showing the average percentage of wound closure ±SE as quantified using ImageJ software. Statistically significant difference in wound closure of compressed PANC-1 cells compared with control cells is indicated with an asterisk (*) ($n \geq 10$; three biological replicates; $P < 0.05$ in Student t test). **G,** Relative mRNA expression of EMT markers *Snail*, *Twist*, *Slug* as quantified by qPCR in MIA PaCa-2 and PANC-1 cells. Each bar indicates the mean fold change ±SE of three independent experiments ($n = 9$). Asterisk (*) indicates a statistically significant difference ($P < 0.05$ in Student t test). **H,** G-LISA was performed to analyze activation of cdc42 and Rac-1 small GTPases in compressed (4.0 mmHg) cells at different timepoints. Assay was performed in triplicates and graphs represent the average fold change ±SE of each protein in compressed relative to uncompressed (control) cells. Asterisk (*) indicates a statistically significant difference ($P < 0.05$ in Student t test).

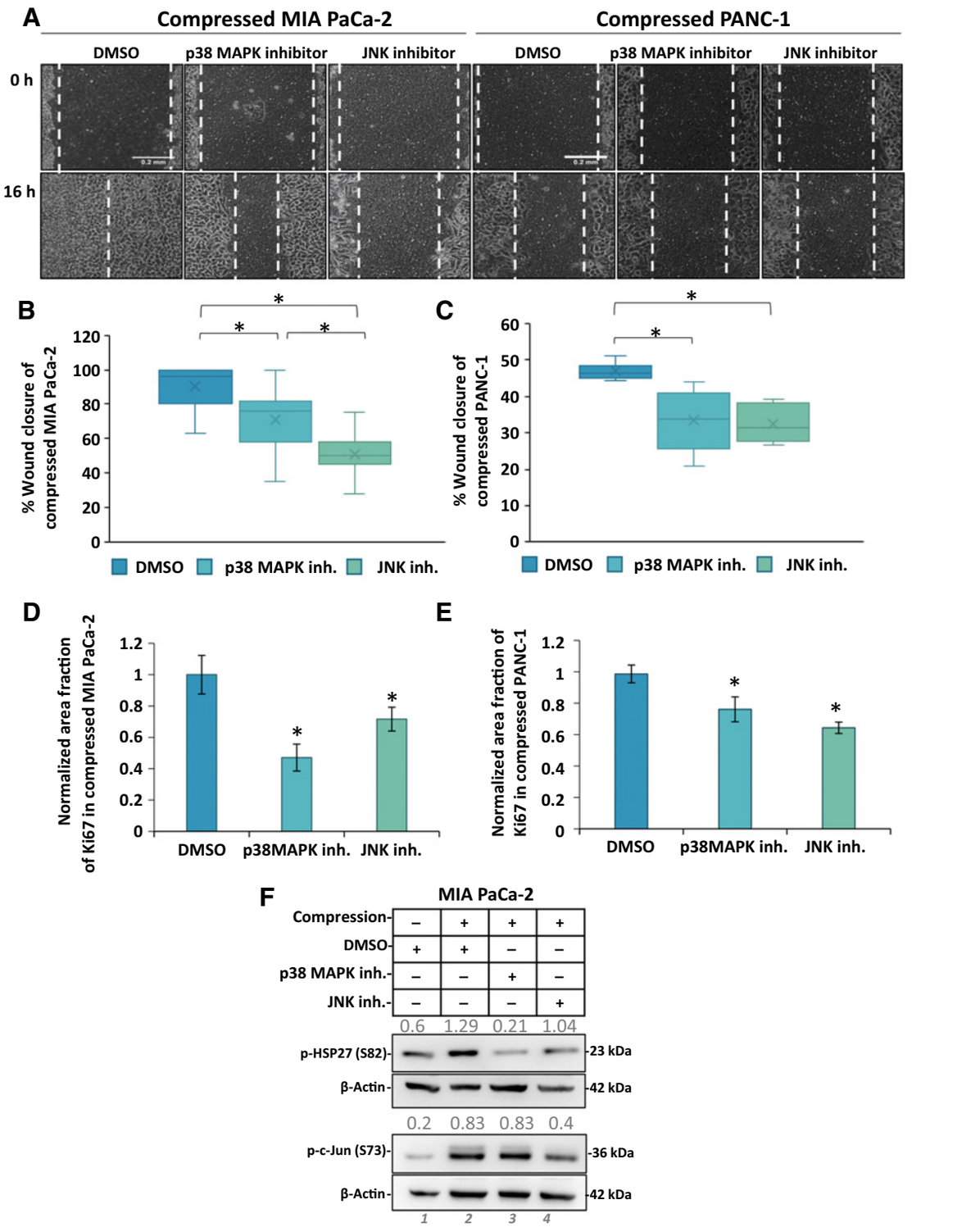

Figure 3.

The p38 MAPK/HSP27 and JNK/c-Jun pathways are necessary for both proliferation and migration of pancreatic cancer cells under mechanical stress. **A,** MIA PaCa-2 and PANC-1 cells were pretreated with 15 μmol/L p38 MAPK inhibitor (SB202190), JNK inhibitor (SP600125) or equal volume of DMSO and subjected to a scratch wound healing assay under 4.0 mmHg of compression. Pictures from at least four different fields were taken from three biological replicates. Scale bar: 0.2 mm. White dashed line shows the difference in wound closure between 0 and 16 hours. Graph showing the average ±SE percentage wound closure of compressed MIA PaCa-2 (**B**) and PANC-1 (**C**) treated with DMSO or inhibitors from three biological replicates ($n \geq 12$). (*Continued on the following page.*)

Among the top 10 upregulated proteins, we observed a strong upregulation of the plasminogen activator inhibitor-1 (PAI-1) that is implicated in actin cytoskeleton organization and cell contraction. The effects of PAI-1 are mediated by downstream activation of myosin II, that interacts with actin filaments to form actomyosin, allowing cell contraction and thus, cell motility and invasion (16, 25–29). Indeed, myosin II was also activated in compressed cells (myosin II_pS1943) as shown in **Fig. 1A**. The increase in expression and phosphorylation of these mediators could contribute to the enhanced migration of cells under mechanical compression (16). On the other hand, mechanical stress downregulated multiple targets of the mammalian Target Of Rapamycin (mTOR) pathway, including the p70-S6K_pT389, Rictor_pT1135, 4E-BP1_pS65 and mTOR_pS2448, which promote protein synthesis and cell growth and proliferation (**Fig. 1A**). To evaluate how mechanical stress alters signaling pathways, we computed pathway scores for nine major pathways (19). We found that multiple protein members of the cell-cycle pathway (p27_pT157, cyclin E1, B1, and D1) and the tuberous sclerosis complex (TSC)/mTOR pathway were reduced. In contrast, protein members of the PI3K/Akt (Akt_pS473, GSK3β_pS9, p27_pT198) and the Ras/MAPK (MEK1_pS217, MAPK_pT202_Y204, p90RSK_pT573, JNK_pT183_Y185, c-Jun_pS73) signaling pathways were elevated (**Fig. 1F**; Supplementary Fig. S4). Collectively, our results show that mechanical stress activates cellular stress response mediators and actin cytoskeleton regulators that may trigger cell motility and impair cell-cycle progression and proliferation.

Mechanical stress induces actin cytoskeleton remodeling and contractility of pancreatic cancer cells promoting their migratory ability

Changes in the actin cytoskeleton organization in compressed MIA PaCa-2 and PANC-1 pancreatic cancer cell lines were evaluated using phalloidin staining. We observed increased stress fibres, filopodia, and lamellipodia formation in both compressed MIA PaCa-2 and PANC-1 (**Fig. 2A** and **B**) compared with uncompressed cells. In line with this, we found a decrease in cell circularity and an increase in the aspect ratio of compressed cells compared with control cells (Supplementary Fig. S5A and S5B). On the basis of myosin II (myosin IIa_pS1943) activation shown in RPPA (**Fig. 1A**), we also performed phospho-myosin II staining and found increased phospho-myosin II levels in both compressed MIA PaCa-2 and PANC-1 cells. Phospho-myosin II was also colocalized with actin filaments in compressed cells (**Fig. 2C** and **D**; Supplementary Fig. S5C and S5D) suggesting increased actomyosin contractility. To evaluate whether these changes in cytoskeleton facilitate cell motility under mechanical stress, we performed a scratch wound assay. We found that compressed PANC-1 cells exhibited increased migratory ability as compared with the uncompressed cells (**Fig. 2E** and **F**), similar to the effect that was previously observed in MIA PaCa-2 cells (16). On the basis of the findings of elongated cell shape and increased migration, we analyzed the expression of epithelial-to-mesenchymal transition (EMT) genes *SNAIL*, *SLUG*, and *TWIST* with qPCR. These genes were consistently upregulated in both cell lines, further verifying the enhanced motility of compressed cells (**Fig. 2G**). Finally, we also examined the activation of Rac1 and cdc42 GTPases that regulate actin cytoskeleton organization for the formation of cell protrusions and actomyosin contractility by inducing myosin II activation (22, 25, 30). Indeed, G-LISA showed that the Rac Family Small GTPase 1 (Rac1) is activated as early as 30 minutes after exposure of cells to compression, while the cell devision cycle 42 (cdc42) GTPase is activated at 16 hours (**Fig. 2H**), suggesting a possible mechanical stress–induced activation of the Rac1/cdc42/myosin II axis. At the same time, a cell viability assay and a Ki67 immunostaining proliferation assay, did not show significant changes in compressed compared with control MIA PaCa-2 and PANC-1 cells for at least 16 hours post-compression (Supplementary Fig. S6). Consistent with the decrease in phosphorylation levels of most of the cell-cycle proteins in cells compressed for 16 hours, cell proliferation was reduced 48 hours post-compression (Supplementary Fig. S6). To evaluate whether compression selectively impacts tumor cells we analyzed previously published RNA-seq datasets of normal cells and found that two gene-ontology processes involving actin cytoskeletal remodeling were significantly enriched in both datasets (Supplementary Table S2). In summary, our results suggest that mechanical stress during the first 16 hours of cell adaptation induces changes in actin cytoskeleton through a Rac1/cdc42/myosin II axis and gene expression alterations to trigger cell migration.

The p38 MAPK/HSP27 and JNK/c-Jun pathways are necessary for the migration of pancreatic cancer cells under mechanical stress

To evaluate whether the activation of the stress response pathway, p38 MAPK/HSP27, and JNK/c-Jun played a role in the increased migratory potential of cells under mechanical stress, we treated MIA PaCa-2 and PANC-1 cells with p38 MAPK (SB202190) or JNK (SP600125) inhibitors. Immunoblotting for phospho-HSP27 and phospho-c-Jun that are downstream of p38 MAPK and JNK, respectively, confirmed effective pathway inhibition for each inhibitor (**Fig. 3F**; Supplementary Fig. S7A). We next performed a scratch wound assay and we observed a significant decrease in the migration of MIA PaCa-2 and PANC-1 cancer cells when treated with either inhibitor under compression (**Fig. 3A–C**), while no effect was observed when uncompressed cells were treated with the same concentration (15 μmol/L) of either inhibitor (Supplementary Fig. S8A and S8B). Cell proliferation was also effectively reduced as revealed by Ki67 staining (quantification in **Fig. 3D** and **E**; Supplementary Fig. S7D). To further confirm our results, we treated cells with siRNAs against *p38 MAPK alpha* and *JNK1/2*. After confirming successful knockdown of each protein (Supplementary Fig. S8C), we performed a scratch wound assay of siRNA-treated control and compressed cells. We observed that only compressed cells that were treated with sip38 MAPK or siJNK1/2 exhibited a decrease in their migratory ability compared with the respective uncompressed cells (Supplementary Fig. S8D). To further support our conclusion, we evaluated EMT markers using qPCR and observed that the expression of *SLUG* and *SNAIL* in MIA PaCa-2 and *SNAIL*, *TWIST* and, to a degree, *SLUG* in PANC-1 is downregulated when cells were treated with either inhibitor (Supplementary Fig. S7B and S7C). Consistent with the reduction in cell migration and the expression of EMT markers, actin cytoskeleton

(*Continued.*) Asterisk (*) indicates a statistically significant difference ($P < 0.05$ in one-way ANOVA analysis). Graph showing the average Ki67 area fraction in compressed MIA PaCa-2 (**D**) and PANC-1 (**E**) cells treated with DMSO, p38 MAPK or JNK inhibitor from at least 10 different fields/condition from two biological replicates as quantified automatically using an in-house code in MATLAB. Asterisk (*) indicates a statistically significant difference in Student *t* test ($P < 0.05$). **F,** Representative immunoblotting showing phosphorylated HSP27 (Ser 82) and c-Jun (S73) in control and compressed MIA PaCa-2 cells treated with 15 μmol/L of each inhibitor or equal volume of DMSO. Antibody against β-actin was used as a loading control. Quantification of each antibody compared with loading control was quantified by ImageJ and it is indicated by numbers in gray font.

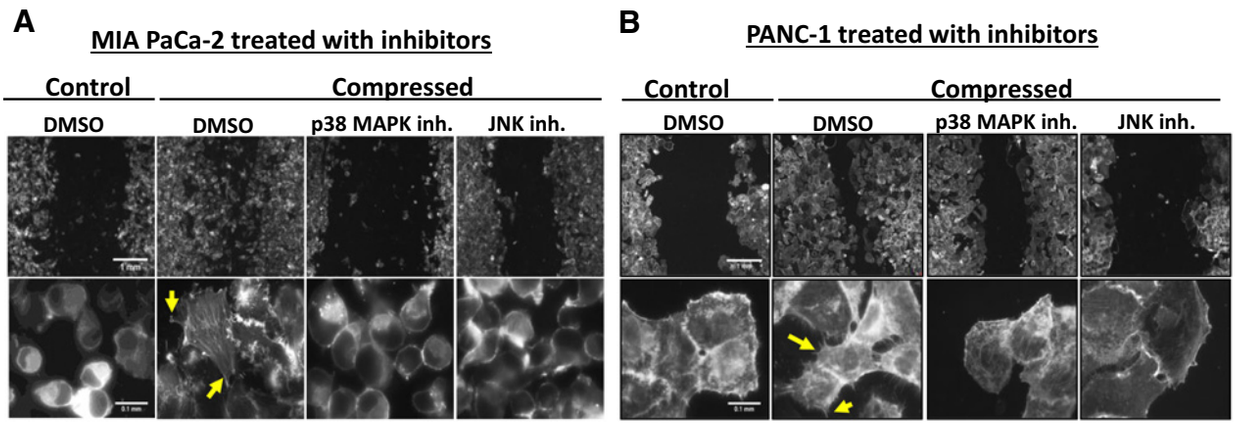

Figure 4.
p38 MAPK/HSP27 and JNK/c-Jun signaling axes promote mechanical stress–induced actin cytoskeleton remodeling. Representative images of phalloidin staining in control and compressed MIA PaCa-2 (**A**) and PANC-1 (**B**) cells treated with DMSO, p38 MAPK or JNK inhibitors. In each panel, the first row shows representative images at the end of the wound healing assay, while the second row shows cells at the wound edge in higher magnification (scale bar: 1 and 0.1 mm, respectively). Yellow arrows indicate cell protrusions (lamellipodia, filopodia) that are necessary for cell migration.

staining in compressed cells treated with either inhibitor showed a reduction in cell protrusions as well as stress fibre formation (**Fig. 4A** and **B**). Quantification of cell morphology showed that cell aspect ratio is decreased, and cell circularity is increased upon treatment of cells with either inhibitor (Supplementary Fig. S9). Collectively, these results suggest that mechanical stress can lead to activation of p38 MAPK and JNK signaling pathways that are necessary for actin cytoskeleton remodeling and cancer cell migration, as well as, to sustain the proliferation of cells under compression.

The Rac1- and cdc42-GTPases mediate mechanical stress–induced cytoskeletal changes that promote pancreatic cancer cell migration

Because mechanical stress induces the formation of cell protrusions, filopodia, and lamellipodia (**Fig. 2A** and **B**), and because these structures are regulated by RAC1 and cdc42 small GTPases (31–33), we treated MIA PaCa-2 and PANC-1 cells with siRNAs against *RAC1* and *CDC42* and performed a scratch wound healing assay and phalloidin staining to examine their role in mediating effects of compression. Once we confirmed the successful knockdown of these genes (**Fig. 5A** and **B**; Supplementary Fig. S10A and S10B), we observed a strong inhibition of wound closure in siRac1–treated cells, and a weaker effect in the sicdc42-treated cells (**Fig. 5C–E**). Consistent with the reduction in migratory potential, knockdown of *RAC1*, and to a lesser extent of *CDC42*, reduced actin stress fiber, filopodia, and lamellipodia formation, as well as cell aspect ratio, and increased cell circularity (**Fig. 6A** and **B**; Supplementary Fig. S10C–S10E). In line with this, we also found that although myosin II was activated in either siRNA-treated compressed cells, there was a reduction in actomyosin formation, evidenced by the reduced myosin II-actin colocalization (**Fig. 6**; Supplementary Fig. S10F and S10G). To determine epistasis between *RAC1* and *CDC42* downregulation and JNK or p38 MAPK activation, we performed immunoblotting. We found that JNK and p38 MAPK activation remained unaffected upon knockdown of either *RAC1* or *CDC42* (Supplementary Fig. S10A). In addition, treatment with either siRac1 or sicdc42 did not affect the proliferation of either MIA PaCa-2 or PANC-1 cells as indicated by Ki67 staining (**Fig. 5F**; Supplementary Fig. S10B). Collectively our results suggest that p38 MAPK and JNK activation in response to mechanical stress that sustains cell viability does not depend on the Rac1 and cdc42 GTPases, while these GTPases are necessary for actin cytoskeleton reorganization and cell motility.

Discussion

Although mechanical stress has already been associated with pancreatic tumor progression and treatment resistance, little is known about the molecular mechanisms involved. To this end, we used RPPA-based proteomic profiling, to examine signaling pathway adaptation in compressed pancreatic cancer cells; we evaluated multiple signaling pathways, such as actin cytoskeleton remodeling, Ras/MAPK, PI3K/AKT, TSC/mTOR, cell-cycle progression, and apoptosis. On the basis of RPPA, we observed an upregulation of the autophagy marker LC3A-B as well as the ER stress sensor, BiP-GRP78. This could be linked with the observation that mechanical compression has recently been suggested to cause mitochondrial dysfunction, leading to autophagy and ER stress response activation through alterations in actin cytoskeleton organization and dynamics (34, 35). Moreover, it has been suggested that both the autophagy and ER stress response could be mediated through p38 MAPK and JNK signaling pathway activation, which are indeed activated in compressed cells (34, 35). Thus, it is possible that mechanical stress can induce cytoskeletal changes, and signaling pathway adaptation that leads to autophagy and ER stress response, which, in turn, promote cell growth and survival under environmental stress. This is also supported by data showing that autophagy could mediate the Ras-driven pancreatic tumor progression and could serve as a marker of poor prognosis for pancreatic tumor patients (30). Notably, the mechanical stress–induced activation of autophagy and ER stress response could also explain that while targets of the mTOR and cell-cycle progression were downregulated or inactivated in compressed cells, the proliferation of compressed cells did not exhibit significant changes compared with uncompressed cells at least 16 hours post-compression (Supplementary Fig. S6).

The most pronounced changes found in RPPA analysis of compressed cells were related to stress response, cell migration, and actin cytoskeleton organization (**Fig. 1**). To this end, and to identify the mechanical stress-induced mechanism that caused those alterations,

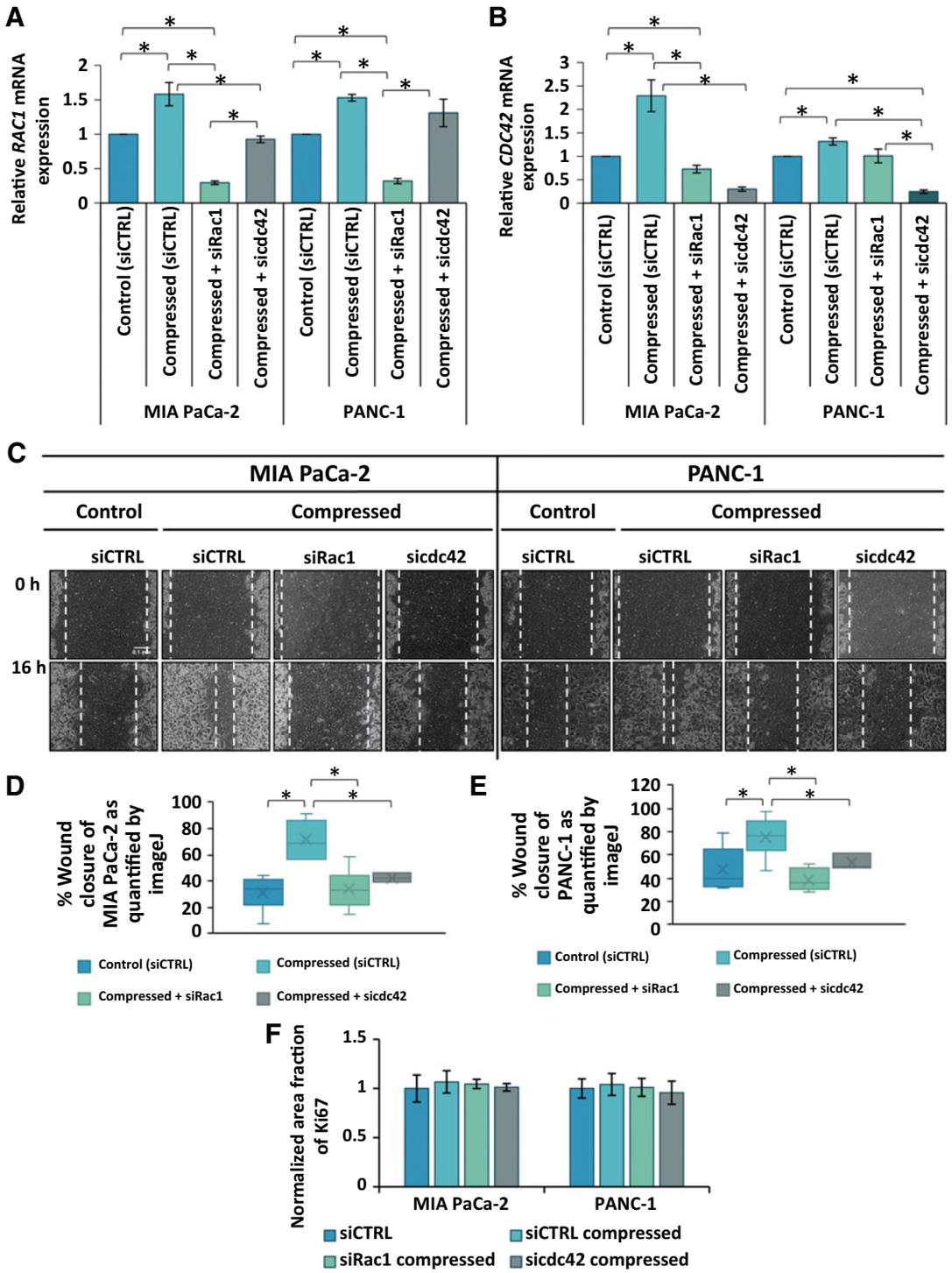

Figure 5.

The Rac-1- and cdc42-small GTPases mediate mechanical stress-induced pancreatic cancer cell migration. Rac1 (**A**) and cdc42 (**B**) mRNA expression was quantified by qPCR in both MIA PaCa-2 and PANC-1. Each bar indicates the mean fold change ±SE of two biological replicates ($n = 6$). Asterisk (*) indicates a statistically significant difference ($P < 0.05$ in one-way ANOVA analysis). **C,** MIA PaCa-2 and PANC-1 pancreatic cancer cells were treated with siRNA against *RAC1* (siRac1) or *CDC42* (sicdc42) and then subjected to a scratch wound healing assay for 16 hours under 0.0 or 4.0 mmHg of compression in 2% FBS containing DMEM. Control cells were treated with stealth siRNA (siCTRL). Scale bar: 0.1 mm. Graphs showing the percentage ±SE wound closure of MIA PaCa-2 (**D**) and PANC-1 (**E**) as quantified using ImageJ software. Statistically significant difference in wound closure of compressed siRac1- or sicdc42-treated cells compared to siCTRL-treated cells is indicated with an asterisk (*) (two biological replicates; $n \geq 6$; $P < 0.05$ in one-way ANOVA analysis). **F,** Graph showing the average ±SE Ki67 area fraction in MIA PaCa-2 and PANC-1 control and compressed cells treated with siCTRL, siRac1, or sicdc42 from at least five different fields/condition from two biological replicates as quantified automatically using an in-house code in MATLAB. No statistically significant changes were observed.

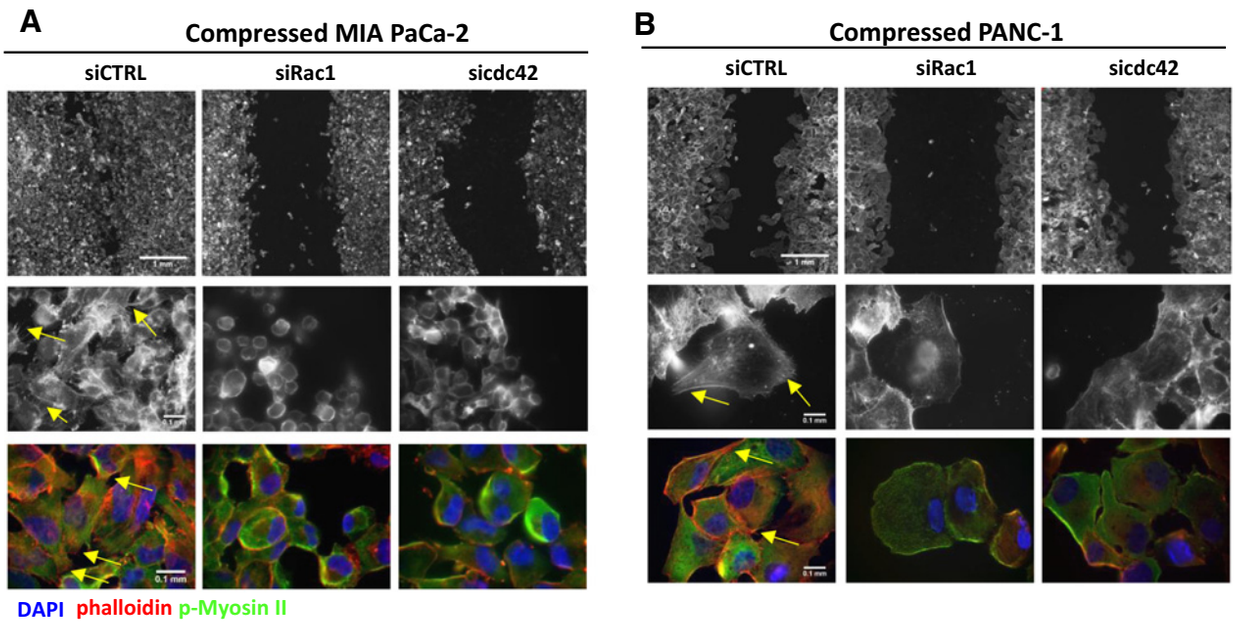

Figure 6.
Rac-1 and cdc42 small GTPases mediate actin cytoskeleton remodeling and contractility to induce cell migration under stress. Representative images of phalloidin and phospho-myosin II (p-myosin II) staining in compressed MIA PaCa-2 (**A**) and PANC-1 (**B**) cells treated with siCTRL, siRac-1, or sicdc42. In each panel, the first row shows representative images at the end of the wound healing assay, while the second row shows cells at the wound edge in higher magnification (scale bar: 1 and 0.1 mm, respectively). Yellow arrows indicate cell protrusions that are necessary for cell migration. Third row shows p-myosin II and phalloidin staining in high magnification (scale bar: 0.1 mm).

we firstly focused on p38 MAPK and its downstream target HSP27, as well as the JNK and its downstream target c-Jun exhibited activation in compressed cells. Although it has already been shown that increased levels of p38 MAPK and JNK activation enhance the efficacy of chemotherapeutic agents, increasing patient survival (15, 25), it is found that both kinases could also lead to increased cancer cell growth, migration, and invasion (15, 36, 37). On a molecular basis, this could depend on the different levels of kinase activity, the duration of its activation, the interaction of the kinase with other signaling pathways as well as cell-type differences. The role of p38 MAPK in cell migration, could be mediated by its downstream target, HSP27, which has been previously shown to promote growth, migration, actin cytoskeleton remodeling, and resistance to chemotherapy in pancreatic tumors and is associated with poor survival (38, 39) for patients with pancreatic cancer (18, 25, 38–40). Similar to p38 MAPK, JNK has also been implicated in cancer cell migration as it has been shown to phosphorylate paxillin to induce the migration and invasion of pancreatic cancer cells (41, 42), while its main downstream target, c-Jun, is expressed in 87% of pancreatic tumor lesions and has been implicated in pancreatic tumor progression (43). To this end, and to further explore whether these molecules are responsible for the increased migratory ability of compressed cells, we first treated MIA PaCa-2 and PANC1 cells with inhibitors for the p38 MAPK and JNK signaling cascades and found that both are necessary for cell migration and proliferation under compression (**Figs. 3** and **4**). Inhibition of these pathways results in more potent reduction of cell migration under compression in our two-dimensional assay (Supplementary Fig. S8D); however whether these pathways synergistically contribute to increased motility requires further investigation in a physiologically relevant three-dimesional setting. In addition, another limitation of our study is whether compressed cells exhibit mechanical memory, as it was recently shown that mechanical stimuli induce epigenetic modifications to regulate cellular behavior (44).

We observed that although mechanical compression did not affect the proliferation of cells within the first 16 hours following force application, when p38 MAPK and JNK were inhibited, there was a reduction in their proliferation. The role of these kinases in cell growth could partially be supported by their contribution in mediating autophagy and ER stress response, events that are necessary for cell adaptation under compression. Regarding their role in cell migration, we further showed that both p38 MAPK and JNK can regulate expression of EMT genes and are necessary for actin cytoskeleton remodeling (**Figs. 3** and **4**). Interestingly, while HSP27 is a downstream target of p38 MAPK that regulates the organization of actin filaments, the disruption of actin cytoskeleton in compressed cells was observed in cells treated with either JNK or p38 MAPK inhibitor. This could be explained by impaired HSP27 activation following JNK inhibition (**Fig. 3**; Supplementary Fig. S7). Although these kinases have been previously reported to have antagonistic effects in cell proliferation and survival (15), it is important to consider the tumor type and their genetic background, as well as the biomechanical cues present in the tumor microenvironment, prior to their targeting for cancer therapy.

Next, based on the increased formation of cell protrusions and myosin II activation observed in compressed cells (**Figs. 1** and **2**), and because Rac-1 and cdc42 small GTPases showed an activation in G-LISA and are known upstream activators of myosin II to facilitate cell motility (45, 46), we downregulated *RAC1* and *CDC42* using siRNAs to examine their role in the mechanical stress–induced migration. Phalloidin and phospho-myosin II staining in

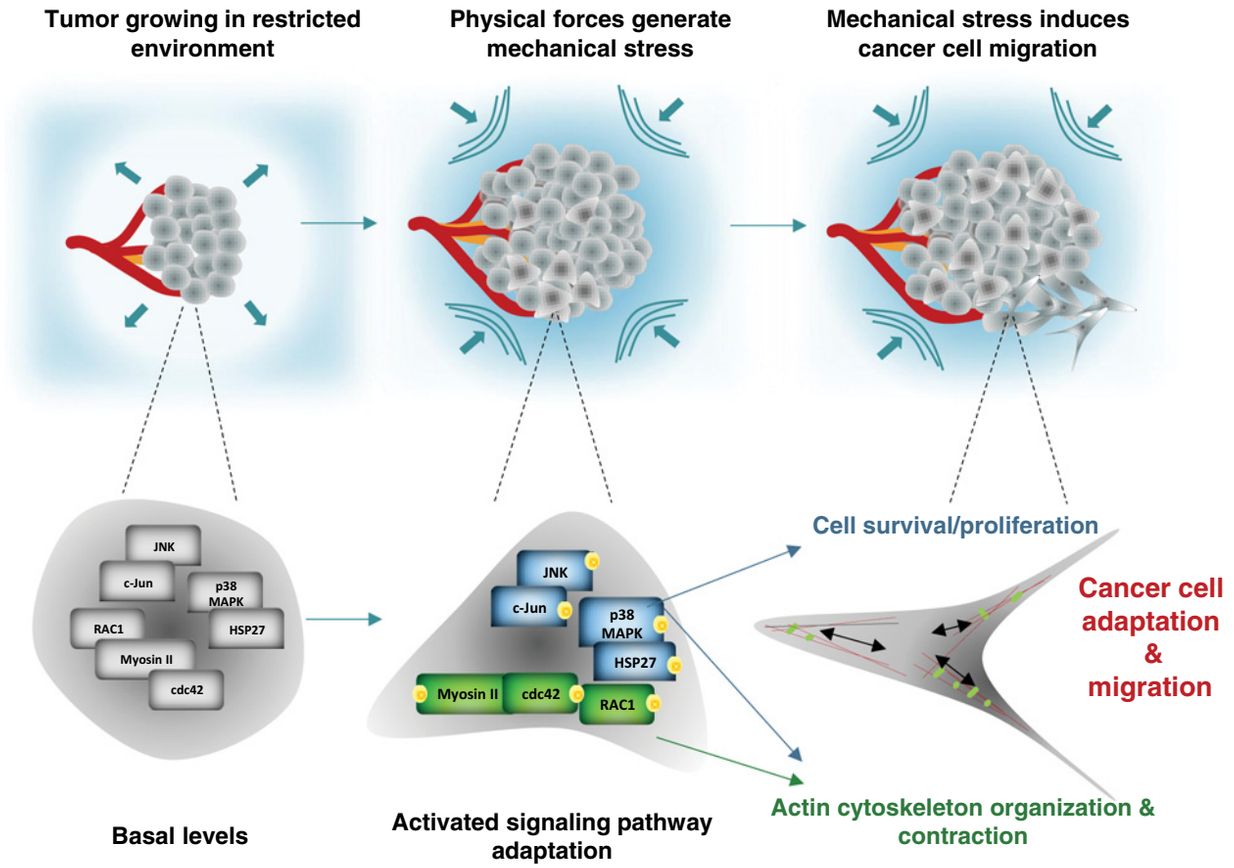

Figure 7.

Mechanical stress–induced signaling pathway adaptation that drives pancreatic cancer cell migration. Mechanical compressive forces are generated during pancreatic tumor growth in the restricted environment of a host tissue. These forces transmit the respective solid stress intracellularly, by activation of JNK/c-Jun, p38 MAPK/HSP27, Rac1, and cdc42. The activation of p38 MAPK/HSP27 and JNK/c-Jun signaling axes can regulate cell adaptation to the new environment by driving their proliferation under compression. Rac1 and cdc42 are activated in turn, and can regulate actin cytoskeleton remodeling for the formation of cell protrusions changing progressively the cell shape. Rac1 and cdc42 also mediate actomyosin contractility, to eventually promote pancreatic cancer cell migration under compression.

compressed siRac1- and sicdc42-treated cells confirmed the role of Rac1 and cdc42 in the formation of cell protrusions and actomyosin contractility, while a scratch wound healing assay revealed that they are all necessary for cell migration under mechanical stress conditions. This effect was less pronounced in sicdc42-treated cells, which exhibited more cell protrusions compared with siRac1-treated cells (Supplementary Fig. S10C). This is further supported by the fact that although cdc42 seems to have an important role in the migration of both control and compressed cells, Rac1 is the key regulator of cell migration under mechanical stress conditions (Supplementary Fig. S11A). This is of particular interest, as increased Rac1 expression is correlated with lower survival rate of pancreatic cancer patients (Supplementary Fig. S11B and S11C). Furthermore, high expression of its downstream effector, phospho-myosin II, is associated with a shorter progression-free survival. These observations highlight that the Rac1/myosin II axis serves as an important adaptation mechanism of compressed cells and a promising target for halting compression-induced metastatic potential.

Collectively, our results, establish a novel mechanism by which mechanical stress enhances tumor progression through the activation of p38 MAPK/HSP27 and JNK/c-Jun signaling axes, and actin cytoskeleton remodelers, Rac1, cdc42, and myosin II (conceptual model shown in **Fig. 7**). Moreover, our proteomic profiling data suggest that cancer cells could survive under mechanical stress conditions through activation of autophagy and ER stress response, indicated by the upregulation of LC3A-B and BiP-GRP78. The high expression of these molecules in pancreatic tumors could be eventually used as a novel marker for the presence of mechanical forces in the tumor interior, and further enhance the importance of targeting mechanically triggered signaling, in combination with conventional treatments, for the cure of pancreatic tumor patients. Therapeutic strategies to alleviate mechanical stresses in tumors have already been developed, with the aim to overcome barriers of effective drug delivery into the highly dense microenvironment of pancreatic and other desmoplastic tumors (47). Our results highlight that targeting aberrant signaling in tumor cells adapting to the mechanical tumor microenvironment presents a novel approach to block tumor migration.

Authors' Disclosures

G.B. Mills is a SAB member/consultant for Abbvie, Amphista, AstraZeneca, Chrysallis Biotechnology, GSK, Ellipses Pharma, ImmunoMET, Ionis, Lilly,

Medacorp, PDX Pharmaceuticals, Signalchem Lifesciences, Symphogen, Tarveda, Turbine, and Zentalis Pharmaceuticals. G.B. Mills reports stock/options/financial interests for Catena Pharmaceuticals, ImmunoMet, SignalChem, Tarveda, and Turbine. G.B. Mills has DSP patents with Nanostring and has licensed a HRD assay to Myriad Genetics. No disclosures were reported by the other authors.

Authors' Contributions

M. Kalli: Conceptualization, formal analysis, investigation, writing–original draft. **R. Li:** Data curation, formal analysis, writing–original draft. **G.B. Mills:** Methodology, writing–review and editing. **T. Stylianopoulos:** Conceptualization, funding acquisition, writing–original draft, writing–review and editing. **I.K. Zervantonakis:** Conceptualization, formal analysis, supervision, funding acquisition, writing–original draft, writing–review and editing.

Acknowledgments

This project has received funding from the European Research Council (ERC) under the European Union's Horizon 2020 research and innovation program (ERC-2018-PoC-838414, ERC-2019-CoG-863955, T. Stylianopoulos), the Department of Bioengineering at the University of Pittsburgh (I.K. Zervantonakis) and NCI (R00 CA222554, I.K. Zervantonakis). G.B. Mills was supported by NCI grant U01 CA217842RPPA was performed by the CCSG supported core at MD Anderson (R50CA221675, G.B. Mills).

The costs of publication of this article were defrayed in part by the payment of page charges. This article must therefore be hereby marked *advertisement* in accordance with 18 U.S.C. Section 1734 solely to indicate this fact.

Received April 11, 2021; revised September 24, 2021; accepted November 4, 2021; published first November 15, 2021.

References

1. Aier I, Semwal R, Sharma A, Varadwaj PK. A systematic assessment of statistics, risk factors, and underlying features involved in pancreatic cancer. Cancer Epidemiol 2019;58:104–10.
2. Stylianopoulos T, Munn LL, Jain RK. Reengineering the physical microenvironment of tumors to improve drug delivery and efficacy: from mathematical modeling to bench to bedside. Trends Cancer 2018;4:292–319.
3. Nia HT, Munn LL, Jain RK. Physical traits of cancer. Science 2020;370: eaaz0868.
4. Provenzano PP, Cuevas C, Chang AE, Goel VK, Von Hoff DD, Hingorani SR. Enzymatic targeting of the stroma ablates physical barriers to treatment of pancreatic ductal adenocarcinoma. Cancer Cell 2012;21:418–29.
5. Chauhan VP, Martin JD, Liu H, Lacorre DA, Jain SR, Kozin SV, et al. Angiotensin inhibition enhances drug delivery and potentiates chemotherapy by decompressing tumour blood vessels. Nat Commun 2013;4:2516.
6. Mpekris F, Papageorgis P, Polydorou C, Voutouri C, Kalli M, Pirentis AP, et al. Sonic-hedgehog pathway inhibition normalizes desmoplastic tumor microenvironment to improve chemo- and nanotherapy. J Control Release 2017;261:105–12.
7. Murphy JE, Wo JY, Ryan DP, Clark JW, Jiang W, Yeap BY, et al. Total neoadjuvant therapy with FOLFIRINOX in combination with losartan followed by chemoradiotherapy for locally advanced pancreatic cancer: a phase 2 clinical trial. JAMA Oncol 2019;5:1020–7.
8. Lawson CD, Burridge K. The on-off relationship of Rho and Rac during integrin-mediated adhesion and cell migration. Small GTPases 2014;5:e27958.
9. Kai F, Drain AP, Weaver VM. The extracellular matrix modulates the metastatic journey. Dev Cell 2019;49:332–46.
10. Stylianopoulos T, Martin JD, Chauhan VP, Jain SR, Diop-Frimpong B, Bardeesy N, et al. Causes, consequences, and remedies for growth-induced solid stress in murine and human tumors. Proc Natl Acad Sci U S A 2012;109:15101–8.
11. Voutouri C, Polydorou C, Papageorgis P, Gkretsi V, Stylianopoulos T. Hyaluronan-derived swelling of solid tumors, the contribution of collagen and cancer cells, and implications for cancer therapy. Neoplasia 2016;18: 732–41.
12. Tse JM, Cheng G, Tyrrell JA, Wilcox-Adelman SA, Boucher Y, Jain RK, et al. Mechanical compression drives cancer cells toward invasive phenotype. Proc Natl Acad Sci U SA 2012;109:911–6.
13. Paul CD, Mistriotis P, Konstantopoulos K. Cancer cell motility: lessons from migration in confined spaces. Nat Rev Cancer 2016;17:131–40.
14. Chen Q, Yang D, Zong H, Zhu L, Wang L, Wang X, et al. Growth-induced stress enhances epithelial-mesenchymal transition induced by IL-6 in clear cell renal cell carcinoma via the Akt/GSK-3beta/beta-catenin signaling pathway. Oncogenesis 2017;6:e375.
15. Wagner EF, Nebreda ÁR. Signal integration by JNK and p38 MAPK pathways in cancer development. Nat Rev Cancer 2009;9:537–49.
16. Kalli M, Minia A, Pliaka V, Fotis C, Alexopoulos LG, Stylianopoulos T. Solid stress-induced migration is mediated by GDF15 through Akt pathway activation in pancreatic cancer cells. Sci Rep 2019;9:978.
17. Kalli M, Voutouri C, Minia A, Pliaka V, Fotis C, Alexopoulos LG, et al. Mechanical compression regulates brain cancer cell migration through MEK1/Erk1 pathway activation and GDF15 expression. Front Oncol 2019;9:992.
18. Kalli M, Papageorgis P, Gkretsi V, Stylianopoulos T. Solid stress facilitates fibroblasts activation to promote pancreatic cancer cell migration. Ann Biomed Eng 2018;46:657–69.
19. Akbani R, Ng PKS, Werner HMJ, Shahmoradgoli M, Zhang F, Ju Z, et al. A pan-cancer proteomic perspective on The Cancer Genome Atlas. Nat Commun 2014; 5:3887.
20. Zervantonakis IK, Iavarone C, Chen H-Y, Selfors LM, Palakurthi S, Liu JF, et al. Systems analysis of apoptotic priming in ovarian cancer identifies vulnerabilities and predictors of drug response. Nat Commun 2017;8:365.
21. Cancer Genome Atlas Research Network. Integrated genomic characterization of pancreatic ductal adenocarcinoma. Cancer Cell 2017;32:185–203.
22. Zhong Y, Naito Y, Cope L, Naranjo-Suarez S, Saunders T, Hong SM, et al. Functional p38 MAPK identified by biomarker profiling of pancreatic cancer restrains growth through JNK inhibition and correlates with improved survival. Clin Cancer Res 2014;20:6200–11.
23. Malm SW, Hanke NT, Gill A, Carbajal L, Baker AF. The anti-tumor efficacy of 2-deoxyglucose and D-allose are enhanced with p38 inhibition in pancreatic and ovarian cell lines. J Exp Clin Cancer Res 2015;34:31.
24. Habiro A, Tanno S, Koizumi K, Izawa T, Nakano Y, Osanai M, et al. Involvement of p38 mitogen-activated protein kinase in gemcitabine-induced apoptosis in human pancreatic cancer cells. Biochem Biophys Res Commun 2004;316:71–7.
25. Even-Faitelson L, Ravid S. PAK1 and aPKCζ regulate myosin II-B phosphorylation: a novel signaling pathway regulating filament assembly. Mol Biol Cell 2006;17:2869–81.
26. Zhang C, Lee HJ, Shrivastava A, Wang R, McQuiston TJ, Challberg SS, et al. Long-term in vitro expansion of epithelial stem cells enabled by pharmacological inhibition of PAK1-ROCK-myosin II and TGF-β signaling. Cell Rep 2018;25: 598–610.
27. Even-Faitelson L, Rosenberg M, Ravid S. PAK1 regulates myosin II-B phosphorylation, filament assembly, localization and cell chemotaxis. Cell Signal 2005;17:1137–48.
28. Prahl LS, Odde DJ. In: Dong C, Zahir N, Konstantopoulos K, editors. Biomechanics in oncology. Springer International Publishing, Cham; 2018. p. 159–87.
29. Nguyen AV, Trompetto B, Tan XHM, Scott MB, Hu KH, Deeds E, et al. Differential contributions of actin and myosin to the physical phenotypes and invasion of pancreatic cancer cells. Cell Mol Bioeng 2020;13:27–44.
30. Fujii S, Mitsunaga S, Yamazaki M, Hasebe T, Ishii G, Kojima M, et al. Autophagy is activated in pancreatic cancer cells and correlates with poor patient outcome. Cancer Sci 2008;99:1813–9.
31. Sun D, Xu D, Zhang B. Rac signaling in tumorigenesis and as target for anticancer drug development. Drug Resist Updat 2006;9:274–87.
32. Keely PJ, Westwick JK, Whitehead IP, Der CJ, Parise LV. Cdc42 and Rac1 induce integrin-mediated cell motility and invasiveness through PI (3) K. Nature 1997; 390:632–6.
33. Yamaguchi H, Lorenz M, Kempiak S, Sarmiento C, Coniglio S, Symons M, et al. Molecular mechanisms of invadopodium formation: the role of the N-WASP–Arp2/3 complex pathway and cofilin. J Cell Biol 2005;168: 441–52.

34. Ong MS, Deng S, Halim CE, Cai W, Tan TZ, Huang RYJ, et al. Cytoskeletal proteins in cancer and intracellular stress: a therapeutic perspective. Cancers 2020;12:238.
35. Blawat K, Mayr A, Hardt M, Kirschneck C, Nokhbehsaim M, Behl C, et al. Regulation of autophagic signaling by mechanical loading and inflammation in human PDL fibroblasts. Int J Mol Sci 2020;21: 9446.
36. Lin M, DiVito MM, Merajver SD, Boyanapalli M, van Golen KL. Regulation of pancreatic cancer cell migration and invasion by RhoC GTPase and Caveolin-1. Mol Cancer 2005;4:21.
37. Taniuchi K, Furihata M, Hanazaki K, Iwasaki S, Tanaka K, Shimizu T, et al. Peroxiredoxin 1 promotes pancreatic cancer cell invasion by modulating p38 MAPK activity. Pancreas 2015;44:331–40.
38. Melle C, Ernst G, Escher N, Hartmann D, Schimmel B, Bleul A, et al. Protein profiling of microdissected pancreas carcinoma and identification of HSP27 as a potential serum marker. Clin Chem 2007;53: 629–35.
39. Schäfer C, Seeliger H, Bader DC, Assmann G, Buchner D, Guo Y, et al. Heat shock protein 27 as a prognostic and predictive biomarker in pancreatic ductal adenocarcinoma. J Cell Mol Med 2012;16:1776–91.
40. Pichon S, Bryckaert M, Berrou E. Control of actin dynamics by p38 MAP kinase–Hsp27 distribution in the lamellipodium of smooth muscle cells. J Cell Sci 2004; 117:2569–77.
41. Cai J, Du S, Wang H, Xin B, Wang J, Shen W, et al. Tenascin-C induces migration and invasion through JNK/c-Jun signalling in pancreatic cancer. Oncotarget 2017;8:74406–22.
42. Ichimaru Y, Sano M, Kajiwara I, Tobe T, Yoshioka H, Hayashi K, et al. Indirubin 3′-oxime inhibits migration, invasion, and metastasis in vivo in mice bearing spontaneously occurring pancreatic cancer via blocking the RAF/ERK, AKT, and SAPK/JNK pathways. Transl Oncol 2019;12:1574–82.
43. Meggiato T, Calabrese F, De Cesare CM, Baliello E, Valente M, Del Favero G. C-JUN and CPP32 (CASPASE 3) in human pancreatic cancer: relation to cell proliferation and death. Pancreas 2003;26:65–70.
44. Watson AW, Grant AD, Parker SS, Hill S, Whalen MB, Chakrabarti J, et al. Breast tumor stiffness instructs bone metastasis via maintenance of mechanical conditioning. Cell Rep 2021;35:109293.
45. Moshfegh Y, Bravo-Cordero JJ, Miskolci V, Condeelis J, Hodgson L. A Trio–Rac1–Pak1 signalling axis drives invadopodia disassembly. Nat Cell Biol 2014; 16:574–86.
46. Surcel A, Schiffhauer ES, Thomas DG, Zhu Q, DiNapoli KT, Herbig M, et al. Targeting mechanoresponsive proteins in pancreatic cancer: 4-hydroxyacetophenone blocks dissemination and invasion by activating MYH14. Cancer Res 2019;79:4665–78.
47. Mpekris F, Panagi M, Voutouri C, Martin JD, Samuel R, Takahashi S, et al. Normalizing the microenvironment overcomes vessel compression and resistance to nano-immunotherapy in breast cancer lung metastasis. Adv Sci 2020;8:2001917.